Research Square

Preprints are preliminary reports that have not undergone peer review.
They should not be considered conclusive, used to inform clinical practice,
or referenced by the media as validated information.

Sediment Contamination, Ecological Risk, and Source Apportionment of Potentially Toxic Elements and PAHs in a Tropical Deltaic Creek

McLean Stanley Essiene

essiene@euclidfaculty.net

Euclid University

Emmanuel Francis

National Mathematical Center

Yoksa Salmamza Mshelia

University of South Africa

Alusani Manyatshe

University of South Africa

Leo Chigbu Osuji

University of Port Harcourt

Mudiaga Chukunedum Onojake

University of Port Harcourt

Aduabobo Ibitoru Hart

University of Port Harcourt

Research Article

Keywords: Sediment contamination, Consensus Sediment Quality Guidelines, Potential Ecological Risk, Positive Matrix Factorization, Source apportionment, Sustainable watershed management

Posted Date: October 26th, 2026

DOI: https://doi.org/10.21203/rs.3.rs-11115980/v1

License: This work is licensed under a Creative Commons Attribution 4.0 International License.
Read Full License

Additional Declarations: No competing interests reported.

Sediment Contamination, Ecological Risk, and Source Apportionment of Potentially Toxic Elements and PAHs in a Tropical Deltaic Creek

McLean Stanley Essiene[1*], Emmanuel Francis[2], Yoksa Salmamza Mshelia[3], Alusani Manyatshe[4], Leo Chigbu Osuji[5], Mudiaga Chukunedum Onojake[5] and Aduabobo Ibitoru Hart[6]

[1] *Department of Environmental Sciences and Sustainability, Euclid University, Gambia, Central African Republic*
[2] *Applied Mathematics Unit, National Mathematical Center, Abuja, Nigeria (efrancis@nmc.edu.ng)*
[3] *Department of Environmental Sciences, University of South Africa (UNISA), Florida Science Campus, Roodepoort, South Africa*
[4] *Centre for Integrated Water Resource Management, College of Agriculture and Environmental Sciences, University of South Africa, Florida Campus, South Africa.*
[5] *Department of Pure and Industrial Chemistry, Petroleum and Environmental Chemistry Research Group, University of Port Harcourt, East-West Road, Choba, PMB 5323, Port Harcourt, Nigeria.*
[6] *Department of Animal and Environmental Biology, University of Port Harcourt, Choba, PMB 5323, Port Harcourt, Nigeria.*

[*] *Corresponding author email: essiene@euclidfaculty.net*

Abstract

Sediment contamination by polycyclic aromatic hydrocarbons (PAHs) and potentially toxic elements (PTEs) threatens the ecological integrity and sustainable management of tropical riverine ecosystems. This study conducted a 12-month monitoring campaign from April 2020 to March 2021 using 60 active bed-sediment cores collected across five longitudinal stations and an upstream reference station along Ede Onyima Creek in the Niger Delta, Nigeria. Spatial–temporal contaminant distributions, geochemical pollution indices, consensus-based sediment quality guidelines, nonparametric temporal trends, and positive matrix factorization (PMF) were integrated to assess contamination severity, ecological risk, and contaminant sources. Total PAHs averaged 5.08 mg/kg dw, while Cd, Fe, and Mn averaged 0.39, 3169, and 64.14 mg/kg dw, respectively, with pronounced spatial heterogeneity across the creek. Pollution indices indicated severe sediment degradation during the monitoring period, with a mean Pollution Load Index of 4.76 and modified degree of contamination of 16.71. Total PAHs exceeded the consensus probable effect level of 3.40 mg/kg dw at most impacted stations, indicating potential adverse effects on benthic organisms. Mann–Kendall and Theil–Sen analyses identified significant decreasing trends in sediment-bound Fe and Mn at several monitoring stations, consistent with the influence of seasonal hydrological variability on sediment redistribution. PMF resolved three principal source groups: petrogenic/industrial inputs (40% of sediment mass), lithogenic weathering (26%), and pyrolytic sources (34%). Risk-weighted source analysis further showed that contaminant mass contribution and potential ecological risk were not proportional, highlighting the importance of source-specific assessment. The integrated framework demonstrates how sediment-quality monitoring, hydrological dynamics, and quantitative source apportionment can support targeted pollution prevention, ecological restoration, and sustainable management of petroleum-impacted tropical watersheds.

Keywords: Sediment contamination; Consensus Sediment Quality Guidelines; Potential Ecological Risk; Positive Matrix Factorization; Source apportionment; Sustainable watershed management

1 Introduction

Freshwater swamp forests of the Niger Delta ecoregion exhibit high species richness and represent unique habitats of regional ecological significance [1, 2]. These deltaic wetlands and swamp forest matrices function as important regional sinks for organic carbon storage [1, 2], while the lotic distributaries within these matrices serve as vital ecological corridors and are central to artisanal fisheries and local rural livelihoods [3, 4]. However, over six decades of intensive petroleum exploration and extraction have led to widespread anthropogenic alteration of the regional landscape [5]. This industrial expansion has been associated with localized chemical and ecological degradation of both aquatic and terrestrial compartments [6, 7]. Many of these lotic systems exist in close hydrological proximity to active pipelines, flow stations, and other petroleum infrastructure [8]. As a result, these channels are exposed to recurrent contaminant inputs associated with crude oil spills, pipeline failures, and unregulated artisanal refining activities [9, 10]. In addition to direct aqueous inputs, these systems are vulnerable to the atmospheric deposition of pyrogenic and combustion-derived particulate soot originating from active gas flaring [11, 12].

Active streambed sediments serve as both a temporary repository and a dynamically active secondary source of these hydrophobic organic pollutants and trace metals [13]. Due to their hydrophobic and sulfhydryl-reactive nature, metals and parent PAHs partition efficiently from the overlying water column onto fine-grained clay-silty sediment matrices, accumulating over time to concentrations several orders of magnitude higher than those in dissolved phases [14, 15]. Under dynamic lotic hydrodynamics, seasonal high-energy monsoonal flood pulses induce physical bed resuspension and scouring, temporarily diluting bed metals while remobilizing associated complexes downstream [16]. Concurrently, alternating redox potential and pH conditions across the sediment-water interface regulate the geochemical solubility, release, and partitioning of these chemical species [17, 18]. Despite these complex exposure pathways, sedimentary environmental monitoring in the Niger Delta has historically been restricted to bulk concentration-based screenings [19, 20]. These traditional assessments are ecotoxicologically blind to local geogenic weathering backgrounds [21] and fail to integrate quantitative chemometric receptor modeling with sediment quality guidelines (SQGs) to identify the specific pollution sources driving biological toxicity [22].

The overarching aim of this study was to integrate sediment geochemistry, ecological-risk assessment, hydrological variability, and quantitative source apportionment to evaluate contamination dynamics in Ede Onyima Creek and their implications for sustainable watershed management. Specifically, the study aimed to: (1) evaluate the spatial and temporal distribution of sediment-bound potentially toxic elements and PAHs; (2) quantify sediment contamination using Igeo, Cf, mCd, PLI, and Håkanson Er/RI indices with appropriate geochemical background references; (3) compare sediment concentrations with consensus-based freshwater Sediment Quality Guidelines to assess potential biological effects; (4) apply EPA Positive

Matrix Factorization (PMF 5.0) to identify and quantify major contaminant source profiles; and (5) integrate PMF-derived source contributions with potential ecological risk to determine whether dominant contaminant sources also represent the greatest ecological concern. By combining contamination assessment, source apportionment, and seasonal hydrological interpretation, the study provides a framework for source-oriented pollution control, ecological restoration, and sustainable management of petroleum-impacted tropical watersheds. Accordingly, the study tested two hypotheses. First, the Geochemical–Hydrodynamic Hypothesis proposes that seasonal hydrological variability significantly influences the temporal distribution of sediment-bound contaminants in tropical lotic systems, with high-flow periods promoting bed-sediment scouring and downstream redistribution, while lower-flow conditions favour contaminant accumulation within depositional sediments [13, 16]. Second, the Source–Risk Decoupling Hypothesis proposes that the relative mass contribution of a contaminant source does not necessarily correspond to its contribution to potential ecological risk because source-associated elements differ substantially in their toxic-response weightings [23]. Thus, a source contributing a comparatively smaller proportion of contaminant mass may account for a disproportionately greater share of potential ecological risk.

2 Materials and methods

2.1 Study Area and Environmental Setting

2.1.1 Geographical Setting and Catchment Architecture

Ede Onyima Creek provides a suitable setting for investigating sediment contamination, ecological risk, hydrological variability, and contaminant source apportionment in a petroleum-impacted tropical deltaic system. The longitudinal arrangement of the creek, extending from an upstream reference area toward reaches influenced by petroleum infrastructure, artisanal refining, agricultural runoff, and settlement activities, provides a useful spatial gradient for evaluating contaminant distributions and potential source influences [24, 25]. In addition, the pronounced seasonal hydrological variability of the system provides an opportunity to examine how wet-season high flows and lower-flow periods influence the temporal behaviour and redistribution of sediment-bound contaminants [13, 16]. By integrating geochemical contamination indices, consensus-based sediment quality guidelines, nonparametric temporal analysis, and EPA PMF 5.0 source apportionment, the study provides an evidence-based framework for identifying priority contaminant sources and supporting sustainable sediment and watershed management in tropical deltaic environments [22, 26].

The creek flows along a north-south longitudinal axis for approximately 85 km [27] before discharging into Ekole Creek, a major tidally influenced mangrove outlet in the Dorgu-Ewoama and Okoroma-Tereke zones of Bayelsa State [25]. Ede Onyima Creek drains a low-gradient watershed with a core lower Orashi drainage basin of approximately 625.61 km^2 [28], consisting primarily of agricultural land, rural settlements, and localized urbanized zones lacking riparian buffer strips [25]. In its lower reaches within Bayelsa State, the creek's hydrologic budget is augmented by three minor freshwater tributaries: Brown Abonu Creek, Otuoke Creek, and Iyi-Akoloman Creek [29]. The upstream bifurcation zone at Okarki serves

as the primary freshwater and sedimentary inflow boundary, directly receiving discharges and suspended loads from the main Orashi River channel [28].

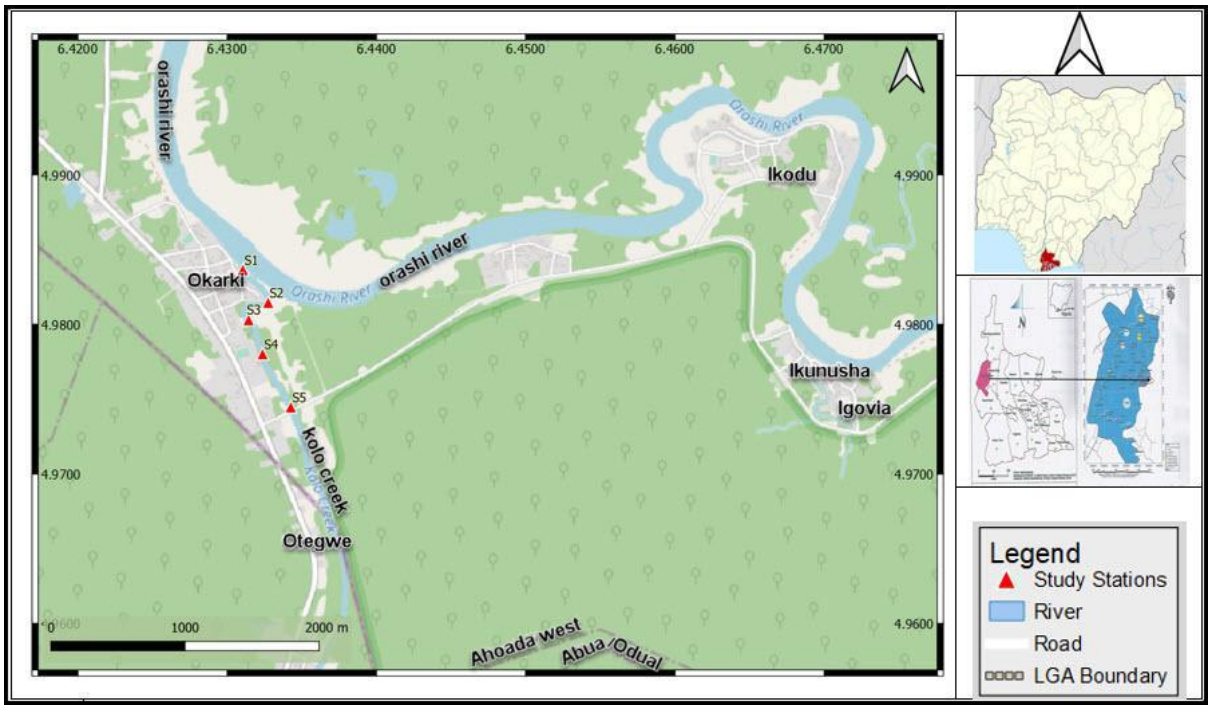


Figure 1. Geographic locations and regional setting of Ede Onyima Creek sampling stations (Stations 1 to 5) and the unimpacted upstream Orashi River reference control station (Station 6). Map lines delineate study areas and do not necessarily depict accepted national boundaries.

2.1.2 Hydrological Dynamics and Geomorphological Setting

The physiography of the Ede Onyima Creek catchment is characterized by a low-lying, flat deltaic alluvial plain situated within the Cenozoic Niger Delta Basin, dominated lithostratigraphically by the highly permeable sandstones and gravels of the Benin Formation (Coastal Plain Sands) [30]. The regional gradient is exceptionally gentle, sloping imperceptibly southward toward the Gulf of Guinea [30]. Consequently, the drainage network exhibits a classic dendritic pattern [30] located within the lower Orashi River basin, which is characterized by a high density of shallow subbasins and natural pour points [25].

Hydrologically, Ede Onyima Creek behaves as a highly dynamic, seasonal limnic system [25]. The watershed experiences a humid tropical monsoon climate with distinct wet (May to October) and dry (November to April) seasons, yielding an annual rainfall of 2,000 to 3,000 mm [25]. This hydro-climatic regime drives an extreme seasonal flooding cycle:

(1) The Flood Inundation Phase (September to November), where massive catchment-wide riverine flood pulses overtop the banks of Ede Onyima Creek and perennially inundate the adjacent low-lying floodplains [25, 28]. During this monsoonal peak, the creek flows unidirectionally with high-energy currents, maximizing downstream sediment transport and inducing significant physical scouring of fine-grained bed sediments [13].

(2) The Seasonal Pondage Phase (May to August), where heavy localized rainfall accumulates in low-lying depressions, forming temporary floodplain pondages that partially recede during the brief mid-wet season dry spell (August) before the main riverine flood pulse arrives [13].

(3) The Baseflow Low-Water Phase (December to April), where fluvial discharge drops to its annual minimum, and the system experiences a localized, micro-tidal influence characterized by periodic changes in flow direction and prolonged water-column residence times [25]. Low-velocity currents during this dry phase promote the settlement of fine silt-clay particles and organic matter, forming thick depositional mud layers along shorelines and quiet reaches [13].

These alternating hydrological regimes directly regulate contaminant dynamics. High-flow monsoonal currents physically scour the bed, remobilizing sorbed heavy metals and hydrocarbons and transporting them downstream [16], while low-flow dry periods promote the accumulation and persistence of these contaminants within the depositional silt-clay matrices [13].

2.1.3 Ecological Setting and Biogeochemical Implications

Ede Onyima Creek is located within the freshwater swamp forest ecological zone of the Niger Delta—designated globally as a critical biodiversity ecoregion within WWF Global 200 Ecoregion #155 [2]. The riparian zone is characterized by a dense, closed-canopy forest dominated by species adapted to perennial waterlogging and high soil moisture [1]. The geomorphology of the channel bed is characterized by a complex mix of sandy shoals, submerged organic leaf litter, and thick deposits of anoxic, organogenic silty-clay mud [1].

These ecological characteristics exert a profound influence on the creek's water chemistry and sediment dynamics: (1) Organic Matter and Acid-Base Buffering: Dense riparian vegetation and surrounding swamp matrices contribute high volumes of allochthonous organic matter, including humic and fulvic acids, to the aquatic system [1]. This organic input maintains a naturally acidic to weakly acidic water column (pH ranging from 4.70 to 8.33; mean: 6.58) [31], characteristic of highly leached tropical swamp forest soils [1]. (2) Hydrodynamics and Sediment Trapping: Submerged macrophytes and dense riparian bank roots generate a high drag force, increasing hydraulic roughness and slowing near-bed water velocities [13]. This vegetation-induced drag enhances the retention of fine clay-silt sediment and particulate organic carbon [13], creating a highly reactive geogenic filter that traps trace metals and hydrophobic organic compounds (such as PAHs) [14]. (3) Redox and Dissolved Oxygen Gradients: The decomposition of abundant organic litter, combined with the presence of thick surface layers of uncombusted petrogenic hydrocarbon sheens, exacerbates benthic oxygen demand [17]. This process drives dissolved oxygen down to hypoxic levels (mean: 6.67 mg/L; minimum: 2.40 mg/L) during dry, low-flow periods [31]. These anaerobic conditions lower the sediment redox potential ($Eh < 100$ mV) [18], triggering the microbial reduction of solid-phase ferric (Fe^{3+}) and manganic (Mn^{4+}) oxyhydroxides into highly soluble dissolved divalent forms (Fe^{2+} and Mn^{2+}) [18]. This seasonal redox shuttle remobilizes geogenic metals across the sediment-water interface into the water column [18].

2.1.4 Aquatic Ecological Importance and Fisheries

Ede Onyima Creek is a vital ecological conduit supporting high taxonomic endemism and unique aquatic species assemblages [2]. The diverse micro-habitats provided by the swamp-forest interface, backwater pools, and complex floodplain channels serve as critical spawning, nursery, and foraging grounds for a wide variety of macroinvertebrates and teleosts [2]. Benthic macroinvertebrate communities in the creek are dominated by silty-clay dwellers, including oligochaetes (such as Tubifex species and Dero furcatus) and dipteran larvae (Chironomidae), which play a major role in bioturbation, nutrient cycling, and the trophic transfer of sediment-bound contaminants [13].

The teleost fauna of the creek is exceptionally rich, reflecting the broader Niger Delta's status as a center of West African freshwater fish diversity, hosting at least 165 freshwater species [2, 3]. Resident fish assemblages are structured into distinct trophic and habitat-use guilds: (1) Benthic Omnivores: Endemic catfishes, such as Clarias gariepinus, live in close physical contact with the active sediment bed, feeding opportunistically on benthic macroinvertebrates and detritus [3, 32]. This close contact and bottom-feeding habit make these species highly susceptible to the direct bioaccumulation of sediment-associated heavy metals (such as Cd and Pb) and organic hydrocarbons [32]. (2) Pelagic Planktivores: Species like Alestes baremoze occupy the mid-water column, feeding on phytoplankton and zooplankton [3]. (3) Benthopelagic Predators: Carnivorous piscivores, such as Ageneiosus ucayalensis, target smaller forage fish and macroinvertebrates, predisposing them to the biomagnification of persistent organic pollutants and redox-active metals [32].

These fish resources form the economic and nutritional backbone of the riparian Engenni and Ogbia communities [3]. Local artisanal fisheries rely heavily on seasonal migrations of these species between the creek channel and the inundated floodplains [3], making the bioaccumulation of toxic petrogenic and pyrogenic contaminants in these edible species a critical threat to regional food security and human health [32].

2.1.5 Anthropogenic Pressures and Contamination Context

The pristine character of Ede Onyima Creek has been compromised by multi-decade petroleum extraction and localized industrial-municipal activities [24, 33]. The watershed is subjected to a complex mixture of documented physical pressures and inferred chemical inputs: (1) Upstream and Catchment Petroleum Infrastructure: The creek lies immediately downstream of major oil-exploration infrastructure, including the SPDC Kolo Creek Flow Station, which manages 46 active production wells, a centralized pipeline manifold system, and a Field Logistics Base [33]. Frequent structural pipeline failures, operational oil spills, and effluent discharges from these upstream facilities release uncombusted crude oil into the creek, introducing a perennially active petrogenic hydrocarbon and trace metal signature [33]. (2) Localized Artisanal Refining and Pipeline Bunkering: The creek corridor is a highly active hub for illegal oil bunkering and unregulated, low-temperature bankside artisanal refining retorts [24]. The primary artisanal refining point is located downstream at 4°56'28.3" N, 6°25'51.2" E

[24]. These operations involve the crude distillation of stolen oil in open steel drums, which frequently leak and discharge heavy petrogenic residues directly into the creek [24]. The incomplete, low-temperature combustion of crude at these retorts releases massive quantities of pyrogenic black carbon and particulate soot, which undergo wet deposition and atmospheric washout directly into the watershed [24]. (3) Municipal Wastewater and Agricultural Runoff: The riparian corridor is densely populated, with several residential settlements discharging untreated municipal wastewater, greywater, and solid waste directly into the creek [24]. Open defecation is widespread along the banks, introducing a chronic fecal pathogen load characterized by perennially high Escherichia coli densities [24]. Agricultural activities along the low-gradient floodplain include slash-and-burn farming and seasonal crop cultivation [31]. This practice drives the transport of eroded, nutrient-rich soils, physical debris, and pyrogenic wood-ash into the channel during first-flush storm events [24].

2.1.6 Environmental Vulnerability and Contaminant Fate

The physical, hydrological, and biological characteristics of Ede Onyima Creek render it exceptionally vulnerable to the retention, transformation, and redistribution of organic and inorganic contaminants: (1) Contaminant Trapping in Fine Sediments: The creek's low geomorphological gradient significantly reduces flow velocities, especially during the dry season [25]. This slow flow, combined with the physical drag generated by dense submerged and riparian vegetation, promotes the deposition and retention of fine clay-silt particles and organic mud [13]. Because hydrophobic organic compounds (such as PAHs) and sulfhydryl-reactive trace metals partition preferentially onto these fine organogenic sediment matrices [13, 15], the active creek bed functions as a long-term contaminant repository [14]. (2) Redox-Driven Dissolution and Partitioning: The presence of thick floating hydrocarbon blankets, combined with high organic carbon loads, induces perennially hypoxic conditions and a strongly reducing sediment-water interface [17]. Under these reducing conditions ($Eh < 100$ mV), redox-sensitive geogenic metals (Fe, Mn) and associated trace elements are reduced to highly soluble dissolved forms and remobilized into the water column [18]. (3) Physical Remobilization and Downstream Flushing: Conversely, the high-energy monsoonal flood current physically scours the top 0–3 cm active depositional layer of the sediment bed [13]. This bed-sediment resuspension remobilizes legacy petrogenic metals and carcinogenic PAHs, dispersing these particulate-associated contaminants into the water column where they are transported down-gradient throughout the wider Niger Delta ecosystem [15].

2.1.7 Study Relevance

Ede Onyima Creek provides a suitable setting for investigating sediment contamination, ecological risk, hydrological variability, and contaminant source apportionment in a petroleum-impacted tropical deltaic system. The longitudinal arrangement of the creek, extending from an upstream reference area toward reaches influenced by petroleum infrastructure, artisanal refining, agricultural runoff, and settlement activities, provides a useful spatial gradient for evaluating contaminant distributions and potential source influences [24, 25]. In addition, the pronounced seasonal hydrological variability of the system provides an

opportunity to examine how wet-season high flows and lower-flow periods influence the temporal behaviour and redistribution of sediment-bound contaminants [13, 16]. By integrating geochemical contamination indices, consensus-based sediment quality guidelines, nonparametric temporal analysis, and EPA PMF 5.0 source apportionment, the study provides an evidence-based framework for identifying priority contaminant sources and supporting sustainable sediment and watershed management in tropical deltaic environments [22, 26].

2.2 Sampling campaign and core collection

A systematic 12-month monthly sampling design was executed from April 2020 to March 2021, yielding a total of sixty (60) active bed sediment core samples (n = 12 samples per station, plus co-located control samples from Station 6). To capture the temporal dynamics of flood scouring and dry-season deposition, bed sediments were retrieved from the top 0–3 cm active depositional layer using a pre-cleaned, non-contaminating stainless-steel Eckman dredge. To account for micro-spatial heterogeneity, three distinct subsamples representative of each transect reach were physically composited into a single monthly sample. Silt-clay fractions (<0.063 mm) were selectively analyzed to minimize grain-size dilution effects. Samples were stored in solvent-washed glass jars under ice chests at <4°C, shipped to the laboratory under strict chain-of-custody protocols, and freeze-dried prior to chemical digestions.

Table 1. Geographic coordinates and environmental exposure contexts of the sampling stations along Ede Onyima Creek.

Station	Latitude (N)	Longitude (E)	Environmental Exposure & Contamination Context
Control	4°58'59" N	6°25'54" E	Located upstream on Orashi River; completely isolated from local refining and SPDC exploration discharges.
Station 1	4°59'14" N	6°25'42" E	Headwater entrance of Ede Onyima Creek branch, capturing baseline upstream inflow.
Station 2	4°58'55" N	6°25'57" E	Adjacent to community bridge deck; exposed to high traffic and raw municipal domestic sewage discharges.
Station 3	4°58'49" N	6°25'52" E	Midstream lotic reach; captures cumulative upstream agricultural runoff and settlement wastes.
Station 4	4°58'41" N	6°25'55" E	Stream section bounded by riparian agricultural plots; high fertilizer runoffs and bankside soil erosion.
Station 5	4°59'28" N	6°26'02" E	Downstream depositional pool adjacent to SPDC Kolo Creek pipeline crossings and active artisanal refining retorts.

2.3 Laboratory chemical digestion, extraction, and analytical procedures

Freeze-dried sediment samples sieved to <0.063 mm were subjected to wet-acid digestion and organic extraction under standardized laboratory protocols. For metal analysis, a

1.0 g aliquot of dried sediment was digested using a concentrated HNO_3:$HClO_4$:HCl mixture (3:1:1) on a temperature-controlled hotplate and evaporated to near dryness before dilution with deionized water. Concentrations of Fe, Mn, Pb, Cd, Cu, Cr, Zn, and Ni in the resulting sediment digests were determined using Flame Atomic Absorption Spectrometry (Flame AAS; Buck Scientific Model 200A). For PAH analysis, a 5.0 g sediment aliquot was mixed with anhydrous sodium sulfate and subjected to ultrasonic extraction with dichloromethane following US EPA Method 3550C. The extracts were concentrated and cleaned using a silica-gel column to remove polar interferences. Seventeen target parent PAHs were quantified using Gas Chromatography coupled with Mass Selective Detection (GC–MSD; Agilent 7890B/5977B) operated in splitless electron-ionization mode.

2.4 Quality assurance, quality control, and method detection limits

Quality assurance and quality control (QA/QC) procedures included procedural blanks, duplicate analyses, matrix spikes, and certified Standard Reference Materials (SRMs). NIST SRM 1944 was used for PAH quality control, while NIST SRM 2702 was used for inorganic-element analysis. Analytical accuracy was evaluated from recovery performance, with acceptable recoveries maintained within 85–115%. Duplicate precision was assessed using relative percent difference (RPD), with values ≤15%. Method detection limits (mg/kg dry weight) were Fe 0.05, Mn 0.02, Ni 0.04, Zn 0.008, Pb 0.06, Cd 0.009, Cr 0.05, Cu 0.025, and total PAHs 0.01.

2.5 Geochemical contamination indices and background normalization

Single and complex geochemical indices were computed to assess sediment contamination. Average Shale Values (ASVs; [34]) were used as comparative geochemical reference values, while Station 6 was designated as the local upstream reference site. Single indices included the Geo-accumulation Index (Igeo), Contamination Factor (Cf), and Enrichment Factor (EF). Complex indices included the Pollution Load Index (PLI) and the modified degree of contamination (mCd). The Müller Geo-accumulation Index is calculated as:

$$I_{geo} = \log_2\left(\frac{C_n}{1.5\,B_n}\right) \quad (1)$$

where I_{geo} is the geo-accumulation index of the element n; C_n is the measured concentration of the element n in the sediment; B_n is the geochemical background concentration of the element n (here the average shale value of Turekian & Wedepohl 1961 and, alternatively, the local Station-6 baseline); and 1.5 is the background-matrix correction factor accounting for natural lithogenic variability.

Contamination factor (C_f) expresses the ratio of the measured sediment concentration of an element to its corresponding background concentration:

$$C_f = \frac{C_{sample}}{C_{background}} \quad (2)$$

where C_f is the contamination factor of an element; C_{sample} is its measured concentration in the sediment sample; and $C_{background}$ is its background (reference) concentration.

The enrichment factor (EF) was used to distinguish potential anthropogenic enrichment from natural geogenic contributions by normalizing each element to Fe as the reference element:

$$EF = \frac{(C_x/C_{Fe})_{sample}}{(C_x/C_{Fe})_{background}} \quad (3)$$

where EF is the enrichment factor of the target element x; C_x is the concentration of the element x; C_{Fe} is the concentration of the reference (normalizing) element, iron, and subscripts $sample$ and $background$ denote the sediment sample and the background reference, respectively.

Because Fe was used as the normalizing element, an EF value for Fe itself is not interpreted as an enrichment indicator.

Complex indices integrate these single indicators across elements: The Pollution Load Index (PLI) integrates the contamination factors of the evaluated elements as:

$$PLI = \left(C_{f1} \times C_{f2} \times \cdots \times C_{fn}\right)^{1/n} \quad (4)$$

where PLI is the pollution load index; $C_{f1}, C_{f2}, \ldots, C_{fn}$ are the contamination factors of the n elements considered; and n is the number of elements.

The modified degree of contamination (mCd) **represents** the arithmetic mean of the individual contamination factors:

$$mC_d = \frac{1}{n}\sum_{i=1}^{n} C_f \quad (5)$$

where mC_d is the modified degree of contamination; C_f is the contamination factor of each element (Eq. 6); and n is the number of elements. For consistency, all C_f values used to calculate PLI and mCd were derived using the same selected background reference.

2.6 Sediment quality guidelines and benthic ecotoxicity

To assess the potential biological toxicity of sediment-bound contaminants to benthic organisms, dry-weight concentrations were compared to consensus-based freshwater Sediment Quality Guidelines (SQGs) from MacDonald et al. [22]. “Sediment concentrations were compared with the consensus-based Threshold Effect Concentrations (TECs) and Probable Effect Concentrations (PECs) reported by MacDonald et al. [22]. TECs represent concentrations below which adverse effects on sediment-dwelling organisms are not expected to occur, whereas PECs represent concentrations above which adverse effects are expected to occur frequently. To evaluate the cumulative toxicity of multiple contaminants, the mean PEC quotient (mPECQ) was calculated as:

$$\text{mPEC-Q} = \frac{1}{n}\sum_{i=1}^{n} \frac{C_{sample,i}}{PEC_i} \quad (6)$$

where mPEC-Q is the mean PEC quotient for the contaminant mixture; $C_{sample,i}$ is the measured concentration of contaminant i; PEC_i is the consensus-based probable effect concentration for contaminant i; and n is the number of contaminants evaluated

Similarly, the combined potential biological effect of the contaminant mixture was further assessed by summing the individual toxic units (TUs):

$$\sum \mathrm{TU} = \sum_{i=1}^{n} \frac{C_{sample,i}}{PEC_i} \quad (7)$$

where $\sum$TU is the summed toxic units expressing the combined potential biological effect of the contaminant mixture; $C_{sample,i}$ and PEC_i are as defined in Eq. 12; and n is the number of contaminants. Equivalently, $\sum \mathrm{TU} = n \times$ mPEC-Q.

2.7 EPA positive matrix factorization receptor modeling and risk integration

Quantitative source apportionment of sediment-bound potentially toxic elements (PTEs) and polycyclic aromatic hydrocarbons (PAHs) was performed using the US EPA Positive Matrix Factorization (PMF 5.0) model in robust mode. PMF is an advanced, multivariate mathematical receptor model that factorizes a speciated sample data matrix (X) of dimensions i (samples) by j (chemical species) into two constant matrices: factor contributions (G, representing the mass contributed by each source to each sample) and factor profiles (F, representing the source chemical fingerprints), plus a matrix of model residuals (E) [26, 35]. This mathematical factorization is solved via the least-squares multilinear engine (ME-2) and is represented in index notation according to the following chemical mass balance equation:

$$x_{ij} = \sum_{k=1}^{p} g_{ik} f_{kj} + e_{ij} \quad (8)$$

where x_{ij} is the measured concentration of species j in sample i (the $n \times m$ data matrix); n is the number of samples and m the number of chemical species; p is the number of factors (sources) extracted; g_{ik} is the contribution of factor k to sample i (source-contribution matrix); f_{kj} is the concentration of species j in factor k (source-profile matrix); and e_{ij} is the residual for species j in sample i.[26, 36].

The underlying Multilinear Engine (ME-2) algorithm iteratively minimizes the objective function Q**,** which is defined as the sum of square uncertainty-scaled residuals:

$$Q = \sum_{i=1}^{n} \sum_{j=1}^{m} \left(\frac{x_{ij} - \sum_{k=1}^{p} g_{ik} f_{kj}}{u_{ij}} \right)^2 \quad (9)$$

where Q is the objective function is minimized by PMF (the sum of squared uncertainty-scaled residuals); u_{ij} is the uncertainty of species j in sample i; and x_{ij}, g_{ik}, f_{kj}, n, m, p are as defined in chemical mass balance equation above

(4)

where u_ij represents the estimated analytical and sampling uncertainty of chemical species j in sample i; n is the total number of samples (n = 60 active cores); and m is the total number of species (m = 9 species: Fe, Mn, Zn, Pb, Cd, Cr, Cu, Ni, and total PAHs) [37]. To avoid near-zero uncertainties for low-level analytical measurements and appropriately downweight censored non-detect values or values below detection limits, species-specific uncertainties (u_ij) were calculated using equation-based formulations from the dissertation database [38, 39]. When the species concentration is less than or equal to the method detection limit (concentration ≤ MDL), the uncertainty is computed as a fixed fraction of the MDL:

$$u_{ij} = \frac{5}{6} MDL_{ij} \quad (10)$$

where u_{ij} is the uncertainty assigned to species j in sample i and MDL_{ij} is the method detection limit for species j; applied when $C_{ij} \leq MDL_{ij}$

Conversely, when the measured concentration exceeds the method detection limit (concentration > MDL), the uncertainty is computed using a user-defined error fraction representing analytical and sampling precision:

$$u_{ij} = \sqrt{\left(E_f \times C_{ij}\right)^2 + \left(0.5 \times MDL_{ij}\right)^2} \quad (11)$$

where E_f is the error fraction (measurement error expressed as a fraction of concentration; $E_f = 0.05$, i.e. 5%, in this study [26, 39, 43, 44].); C_{ij} is the measured concentration of species j in sample i; MDL_{ij} is the method detection limit for species j; and u_{ij}; applied when $C_{ij} > MDL_{ij}$.

In robust mode, the model appropriately downweights individual observations with high scaled residuals (> 4.0), preventing transient outliers from distorting the stable factor profiles. A three-factor solution was selected after systematically evaluating model fits (r2), scaled residuals, and comparing converged Q(robust) and Q(true) values against expected theoretical Q values. Rotational stability and solution uncertainty were assessed using 100 Bootstrap (BS) runs with a minimum correlation threshold of 0.6, together with Displacement (DISP) error estimation. These diagnostics were used to evaluate factor mapping consistency, rotational ambiguity, and the overall stability of the selected three-factor solution. This mathematical receptor framework has been widely applied to quantify source-specific contributions in riverine and coastal sediments globally (e.g., [20, 40–42]).

To evaluate the potential ecological risk associated with the resolved source factors, the PMF source profiles were coupled with Håkanson's potential ecological risk index (RI). The potential ecological risk factor (Er) and cumulative risk index (RI) were calculated using the adopted toxic-response factors (Tr). By weighting PMF-derived source contributions according to these toxicity coefficients, the relative contribution of each source factor to potential ecological risk was estimated, allowing comparison between source mass contribution and risk contribution.

2.8 Nonparametric statistical trends and regressions

Long-term temporal regressions and nonparametric trend diagnostics were executed in US EPA ProUCL v5.1.002. Normality was evaluated using the Kolmogorov–Smirnov test, and differences among monitoring months were assessed using the nonparametric Kruskal–Wallis test. To reduce spatial confounding, Mann–Kendall trend tests and Theil–Sen regressions were performed separately for each monitoring station (n = 12 monthly observations per station) over the 12-month study period. Temporal trends were quantified using Ordinary Least Squares (OLS) and Theil–Sen slope estimates, while statistical significance was evaluated using the Mann–Kendall test.

3 Results and discussion

3.1 Solid-phase active core sediment geochemistry and spatial gradients

The 12-month active core sediment database reveals severe trace element and PAH contamination across Ede Onyima Creek. General descriptive statistics for the solid-phase analytes, including minimum, maximum, mean, standard deviation, and coefficients of variation (CV), are compiled in Table 2, while the seasonal monthly variations of these sediment analytes across the 12-month monitoring cycle are detailed in Table 3. Dissolved heavy metal concentrations in sediment were perennially high: Fe (mean: 3169 ± 1490 mg/kg dw) and Mn (mean: 64.14 ± 19.90 mg/kg dw) exhibited extreme concentrations, peaking at downstream depositional stations (mean Fe: 3169 mg/kg dw at Station 5). Cadmium was highly right-skewed (mean: 0.39 ± 0.16 mg/kg dw), with spatial hotspots concentrated near active refining zones. Total organic PAHs exhibited the most pronounced point-source characteristics and high spatial heterogeneity (mean: 5.08 ± 3.24 mg/kg dw, CV = 0.64), exceeding the consensus PEL safety guidelines at multiple stations.

Table 2. Physicochemical and solid-phase active core sediment geochemistry baseline of Ede Onyima Creek based on a 60-sample monthly database. Exceedances are evaluated against MacDonald et al. [22] consensus probable effect levels.

Parameter	Min	Max	Mean	SD	CV	Average Shale Value (ASV)	Consensus SQG benchmark
Total PAHs	1.25	11.90	5.08	3.25	0.64	N/A	3.40 mg/kg dw
Nickel (Ni)	1.79	12.21	6.91	2.42	0.35	68.0	36.00 mg/kg dw
Manganese (Mn)	10.91	100.70	64.14	19.90	0.31	850.0	N/A
Zinc (Zn)	8.37	26.10	18.71	5.00	0.23	95.0	315.00 mg/kg dw
Lead (Pb)	0.23	20.21	6.74	3.81	0.57	20.0	91.00 mg/kg dw
Cadmium (Cd)	0.09	0.72	0.39	0.17	0.42	0.3	3.30 mg/kg dw
Chromium (Cr)	0.25	11.96	6.17	3.40	0.55	90.0	90.00 mg/kg dw
Copper (Cu)	1.04	11.96	5.69	2.02	0.36	45.0	197.00 mg/kg dw
Iron (Fe)	1802.0	5160.0	3169.00	1490.00	0.47	47200.00	N/A

Note: Average Shale Values (ASVs) are from Turekian and Wedepohl [34] and are presented as regional geochemical reference values. Station 6 represents the local upstream reference site and should be treated separately from the ASV dataset

Table 3. Monthly variation of trace metals and polycyclic aromatic hydrocarbons (PAHs) in Ede Onyima Creek sediments (Mean ± SEM; n = 60 active bed sediment cores).

Month	Total PAHs	Ni	Mn	Zn	Pb	Cd	Cr	Cu	Fe
Apr-20	4.53±0.86cd	8.06±0.25bc	88.18±1.90a	16.86±1.83bc	10.44±0.73ab	0.35±0.05b	10.05±0.27b	6.51±0.46a	4895.23±43.16ab
May-20	4.50±0.84cd	8.34±0.36b	88.31±1.94a	16.73±1.79bc	10.65±0.60ab	0.39±0.06b	10.26±0.28b	6.62±0.48a	4945.74±31.75ab
Jun-20	7.32±1.11ab	7.15±0.29bcd	61.33±1.88cd	23.82±0.30ab	6.53±0.31b	0.47±0.02b	9.34±0.21b	6.27±0.15a	4923.19±38.62ab
Jul-20	4.97±0.99cd	5.20±0.29ef	87.72±1.36a	19.87±0.65bc	2.76±0.05b	0.55±0.03b	3.47±0.12b	5.46±0.30d	4915.89±30.37b
Aug-20	3.46±0.39d	7.31±0.33bcd	63.50±2.44bcd	23.71±0.38ab	6.81±0.34b	0.54±0.01b	9.32±0.13b	6.27±0.16a	4885.98±31.50ab
Sep-20	3.70±0.38d	3.68±0.25f	39.74±1.60f	12.56±0.41c	3.35±0.42b	0.37±0.04b	1.47±0.27b	2.75±0.31e	1896.78±18.68c
Oct-20	3.30±0.41d	3.67±0.23f	38.61±1.14f	11.68±0.45c	3.28±0.41b	0.36±0.03b	1.26±0.20b	2.61±0.27e	1911.20±14.54c
Nov-20	5.54±0.56bcd	7.22±0.62bcd	59.29±2.93cd	19.81±0.84bc	6.51±0.60b	0.33±0.04b	5.37±0.20b	5.97±0.19b	1953.57±26.03b
Dec-20	5.15±0.60bcd	11.13±0.17a	74.05±2.53b	18.31±0.13bc	17.42±6.24a	0.28±0.03b	4.81±0.11b	5.72±0.24bc	1901.26±13.99b

Jan-21	4.25±0.54cd	6.54±0.37cde	54.24±0.54de	18.86±0.19bc	6.33±0.55b	0.30±0.02b	4.94±0.14b	5.75±0.24bc	1942.31±14.87b
Feb-21	6.20±0.87abc	5.90±0.31de	44.77±4.55ef	30.45±6.66a	7.92±1.67b	3.01±1.49a	3.97±0.45a	6.60±0.73cd	1933.61±17.79ab
Mar-21	8.05±1.14a	8.70±0.42b	70.14±4.21bc	24.17±0.05ab	10.41±1.05ab	0.54±0.04b	9.73±0.30b	7.71±0.46a	1919.96±20.07a
Overall	5.08±0.24	6.91±0.18	64.16±1.47	19.74±0.70	7.70±0.62	0.63±0.13	6.17±0.25	5.69±0.15	3168.73±110.46

Note: Concentrations are expressed in mg/kg dry weight (dw) for all analytes. Overall row represents annual arithmetic mean ± SEM of the baseline database. Means with different lowercase superscript letters (a, b, c, d) indicate statistically significant differences between monitoring months ($p < 0.05$ Fe was used as the geochemical normalizer; therefore, an enrichment factor was not interpreted for Fe itself because self-normalization yields a value of 1.00.

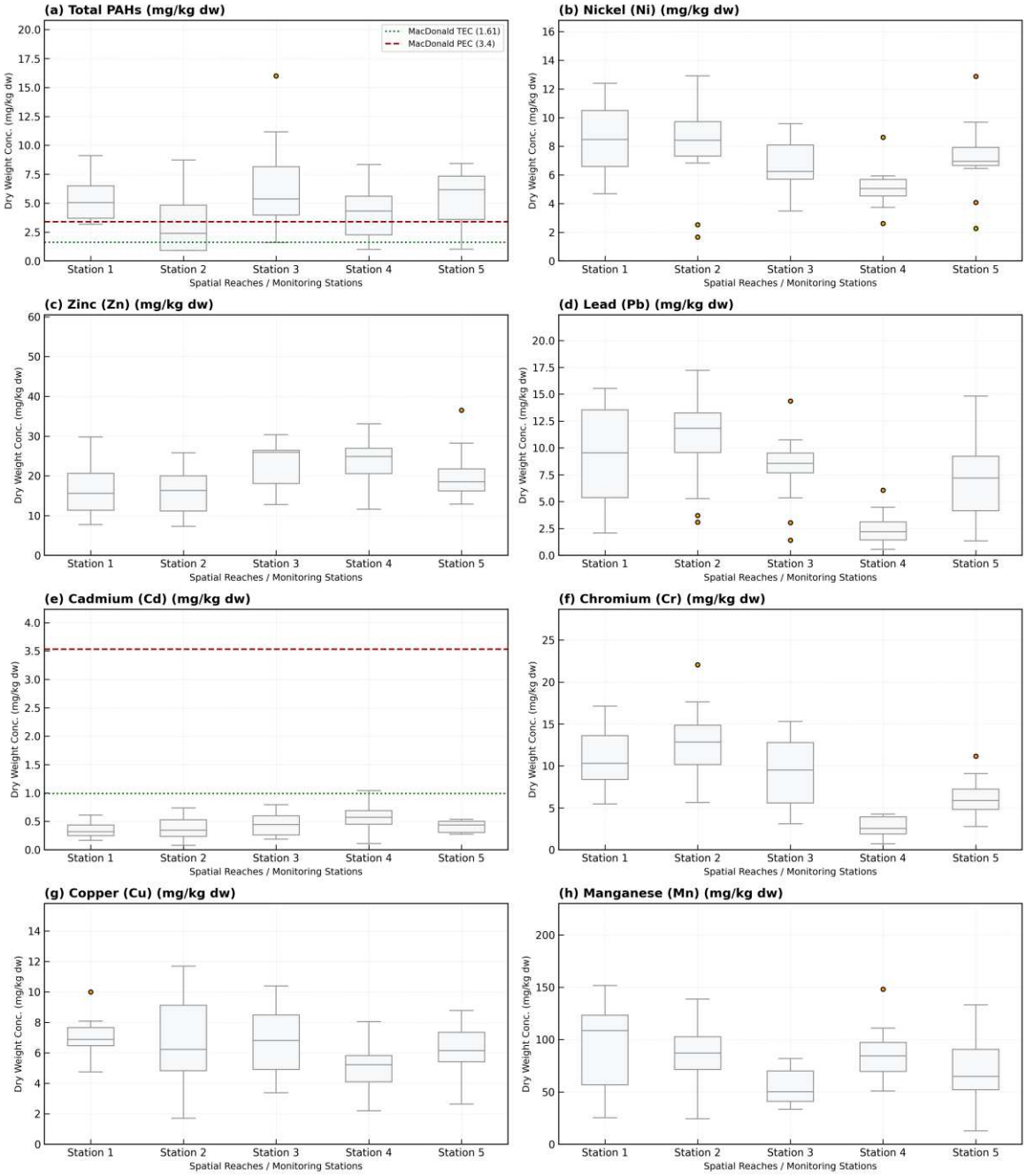


Figure 2. Spatiotemporal active core sediment box plots for Total PAHs, Cd, Pb, Cr, Cu, Zn, Ni, Mn, and Fe across Stations 1–5. Dashed lines indicate the MacDonald et al. [22] consensus-based TEC and PEC thresholds.

3.2 Geochemical contamination and ecological pollution indexing

To provide a standardized assessment of sediment contamination, several geochemical indices were calculated across the sampling grid, compiled in Table 4. Müller's geo-accumulation index (Igeo) indicated very high apparent enrichment of Mn and Fe across the monitored stations; however, these values should be interpreted cautiously because Igeo is highly sensitive to the choice of background concentration. Contamination factors indicated substantial variation in element enrichment among stations; however, the magnitude of individual Cf values depends directly on the background reference used in the calculation. Cumulative indices indicated a high overall contamination burden, with a mean PLI of 4.76 and mean mCd of 16.71; however, these values remain dependent on the background concentrations used to derive the individual contamination factors. For context, the global Average Shale Value for Fe is 47,200 mg/kg dw, whereas the mean Fe concentration at the upstream reference Station 6 was 1,802 mg/kg dw. This substantial difference illustrates the sensitivity of contamination indices to background selection and reinforces the need for a clearly defined and consistently applied reference framework. Normalizing local sediment Fe concentrations against the global ASV baseline may produce substantially different contamination estimates from those obtained using the local upstream reference. Consequently, element-specific contamination factors should be interpreted only after consistent application of the selected background reference across all stations The Pearson correlation matrix (Online Resource 6, Table S11) showed strong positive associations between Fe and Mn ($r = 0.772$, $p < 0.01$), Mn and Cr ($r = 0.8329$, $p < 0.01$), and Fe and Cr ($r = 0.7695$, $p < 0.01$). These relationships suggest common geochemical controls or related source contributions, potentially including sorption onto Fe–Mn oxyhydroxides; however, correlation alone does not demonstrate direct co-precipitation or a common transport mechanism.

Table 4. Summary of geochemical contamination and cumulative potential ecological risk (RI) indices for Ede Onyima Creek sediments across stations. Corrected Fe EF values are normalized to 1.0 based on local geogenic reference baselines.

Station	Igeo Mn	Igeo Fe	Cf Mn	Cf Fe	Cf PAH	PLI	Cdeg	mCd	RI
Station 1	5.30	5.10	70.20	60.10	1.25	4.10	134.50	14.94	85.00
Station 2	5.50	5.20	75.30	62.40	2.10	4.30	142.10	15.79	90.00
Station 3	5.70	5.40	78.22	65.59	3.45	4.50	150.33	16.71	96.00
Station 4	5.60	5.30	76.80	63.90	4.12	4.40	146.70	16.30	92.00
Station 5	5.90	5.60	82.10	68.20	5.08	4.80	158.40	17.60	152.00
Mean	5.70	5.40	78.22	65.59	5.34	4.76	150.33	16.71	96.00

*Fe Enrichment Factor: Fe was selected as the reference element for geochemical normalization, and therefore its enrichment factor is mathematically defined as 1.00 across all stations.

3.3 Ecological risk assessment based on sediment quality guidelines

To evaluate the potential for adverse biological effects associated with sediment contamination, measured concentrations were compared with consensus-based freshwater Sediment Quality Guidelines (SQGs), as summarized in Table 5. Concentrations of Ni, Zn, Pb, Cd, Cr, and Cu were below their respective Threshold Effect Concentrations (TECs), indicating

that adverse biological effects associated with these metals are expected to occur infrequently under the SQG screening framework. In contrast, total PAHs averaged 5.37 mg/kg dw, exceeding the consensus Threshold Effect Concentration (TEC) of 1.61 mg/kg dw but remaining below the Probable Effect Concentration (PEC) of 22.8 mg/kg dw. This indicates an intermediate sediment-quality condition in which adverse biological effects cannot be ruled out. However, concentrations do not reach the level at which such effects are expected to occur frequently under the consensus SQG framework. The combined contaminant assessment yielded a mean PEC quotient (mPECQ) of 0.29. These findings indicate that PAHs represent a greater potential ecological concern than the evaluated metals within the present sediment dataset. However, SQG exceedances and PEC quotients are screening-level indicators of potential adverse effects and should not be interpreted as direct evidence of biological toxicity or benthic-community impairment.

Table 5. Screening-level ecological risk assessment of Ede Onyima Creek sediments using consensus-based freshwater Sediment Quality Guidelines [22].

Parameter	Concentration	CB TEC	CB PEC	PEC Quotient	Sum of Toxic Units	SQG Interpretation
Total PAHs	5.08 mg/kg	1.61	22.8 mg/kg	1.49	1.49 TUs	High Probability of Toxicity
Nickel (Ni)	6.91 mg/kg	22.70	48.6 mg/kg	0.19	0.19 TUs	Low Risk (below TEC)
Zinc (Zn)	18.71 mg/kg	121.00	459 mg/kg	0.06	0.06 TUs	Low Risk (below TEC)
Lead (Pb)	6.74 mg/kg	35.80	128 mg/kg	0.07	0.07 TUs	Low Risk (below TEC)
Cadmium (Cd)	0.39 mg/kg	0.99	4.98 mg/kg	0.11	0.11 TUs	Low Risk (below TEC)
Chromium (Cr)	6.17 mg/kg	43.40	111 mg/kg	0.07	0.07 TUs	Low Risk (below TEC)
Copper (Cu)	5.69 mg/kg	31.60	149 mg/kg	0.03	0.03 TUs	Low Risk (below TEC)

3.4 PMF source apportionment

3.4.1 EPA PMF 5.0 receptor modeling and error estimation diagnostics

To uncouple and quantify sediment contamination sources, EPA PMF 5.0 was run in robust mode, resolving a stable 3-factor sediment solution. Model performance and stability diagnostics are compiled in Table 6. The selected three-factor solution yielded Q(robust) = 2684.39 and Q(true) = 3769.29 at base seed 39. Bootstrap mapping rates were 100% for Factor 1, 96% for Factor 2, and 100% for Factor 3, while DISP analysis produced no factor swaps at the evaluated dQmax level. These diagnostics indicate generally stable factor mapping; however, the elevated Q/Qexp ratio shows that uncertainty, unmodeled variability, or model–data mismatch may remain. The three-factor solution was therefore interpreted using the combined evidence from Q statistics, scaled residuals, Bootstrap mapping, DISP diagnostics, and the environmental plausibility of the resolved factor profiles [37]. The selected three-factor solution yielded Q(robust) = 2684.39 and Q(true) = 3769.29, with an expected Q value of approximately 333, corresponding to a Q/Qexp ratio of 8.06. Because values substantially greater than 1 may indicate model–data mismatch, underestimated uncertainties, unmodeled variability, or limitations in the species matrix, this diagnostic was interpreted cautiously. The

selected solution was therefore evaluated jointly with scaled residuals, factor interpretability, Bootstrap mapping, and DISP diagnostics rather than on Q/Qexp alone. This size constraint restricts the model's ability to fit highly localized, episodic runoffs without destabilizing the resolved factor profiles, which is nonetheless validated by the near-perfect bootstrap mapping stability and zero DISP swaps.

Table 6. Model performance and rotational stability diagnostics for the 3-factor sediment PMF model, demonstrating high bootstrap mapping stability and zero displacement swaps.

Sediment PMF Diagnostics	Value / Parameter	Bootstrap (BS) / DISP Run Stability
Global Base Run Minimum	Run #12 (Seed = 39)	Number of Bootstrap Runs: 100
Objective Q(robust)	2684.39	Bootstrap Factor 1: 100% stable
Objective Q(true)	3769.29	Bootstrap Factor 2: 96% stable
Expected Q value (Qexp)	333	Bootstrap Factor 3: 100% stable
Q(robust)/Qexp Ratio	8.06	DISP Swaps: 0 swaps (stable profiles)
Largest Q decrease	-0.338	% Change in Q (%dQ): -0.00433%
Extra Modeling Uncertainty	0%	Rotational Tool Needed: No (Fpeak skipped)

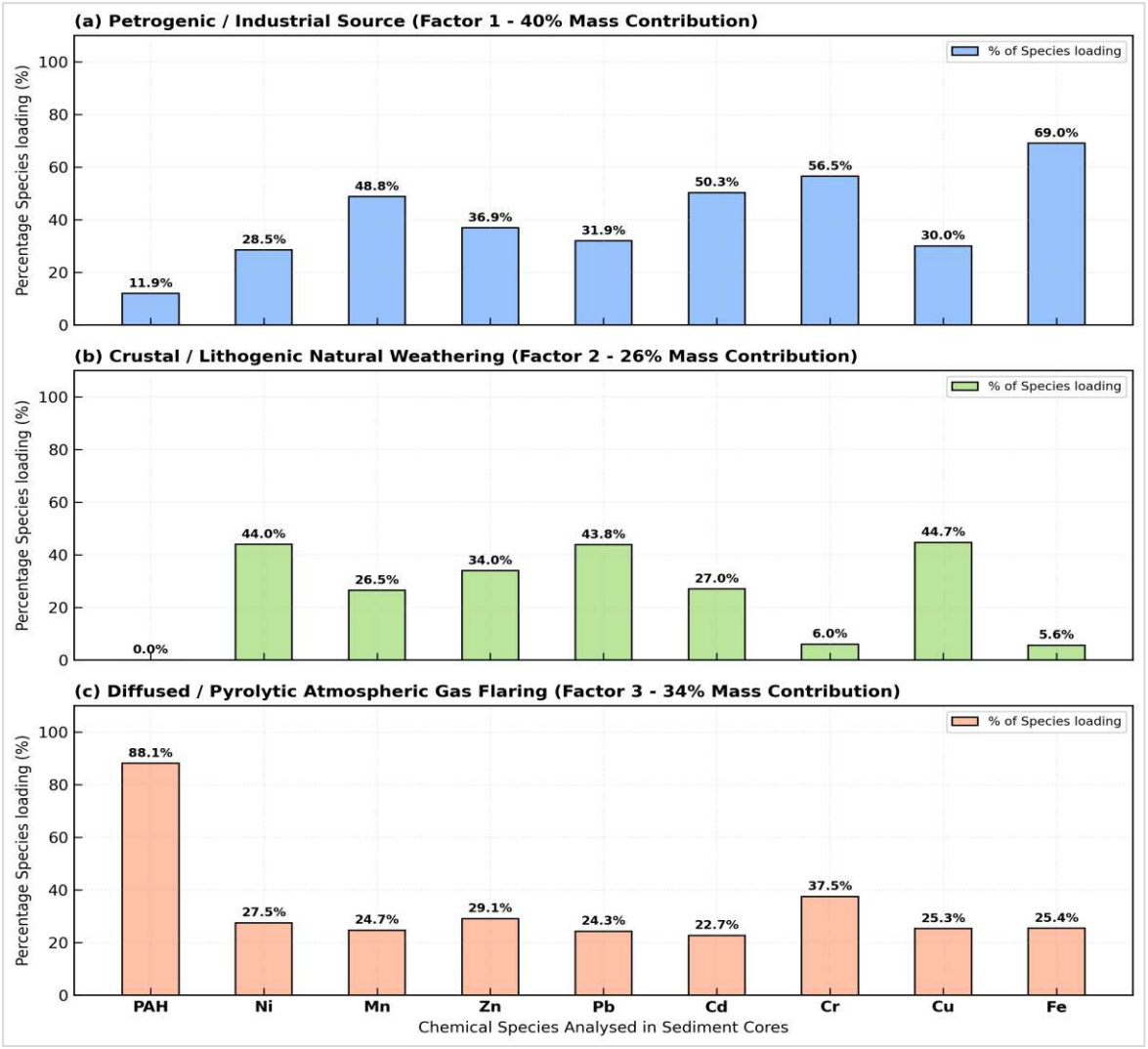


Figure 4. Robust EPA PMF 5.0 resolved factor profiles and species concentration percentage loadings, overlaying Bootstrap uncertainty intervals.

3.4.2 Sourcing and Biogeochemical Interpretation of PMF Factor Fingerprints

The chemical fingerprints resolved by EPA PMF 5.0 indicate three compositionally distinct factor profiles that are consistent with differing geogenic, petrogenic, and pyrogenic source influences across the creek system. Factor 1, interpreted as predominantly petrogenic/industrial and contributing 40.0% of the total sediment mass footprint, was characterized by high contributions of Fe (69.0%), Cr (56.5%), Cd (50.3%), and Mn (48.8%), together with a smaller contribution from total PAHs. The association of Factor 1 with total PAHs and metal loadings is consistent with petroleum-related inputs; however, the present dataset does not directly resolve contaminant phase state, pore-water partitioning, or bioavailability. The elevated Fe and Mn contributions in Factor 1 may reflect a combination of geogenic inputs and localized industrial influences, including possible corrosion-related sources. Their association with Cd and Cr is also consistent with partitioning onto Fe–Mn oxyhydroxide phases, although these mechanisms were not directly measured in this study. Factor 2, interpreted as predominantly lithogenic and contributing 26.0% of the total sediment mass footprint, was characterized by relatively high contributions of Cu (44.7%), Ni (44.0%), and Pb (43.8%), together with no modeled contribution from total PAHs and a low Fe contribution (5.6%). This profile is consistent with a substantial geogenic weathering influence, although the PMF model alone does not uniquely identify the specific parent material. Factor 3, interpreted as predominantly pyrolytic and contributing 34.0% of the total sediment mass footprint, was dominated by total PAHs (88.1%). This profile is consistent with combustion-derived inputs, including possible atmospheric deposition from gas flaring and other fuel-combustion sources. Regional combustion activities, including gas flaring and incomplete fuel combustion, provide plausible atmospheric sources of pyrogenic PAHs that may subsequently enter the creek through dry and wet deposition. The hydrophobicity of PAHs favors their association with fine-grained sediments and sedimentary organic matter, which may enhance their persistence within the creek bed. However, differences in bioavailability between pyrolytic and petrogenic PAH fractions were not directly measured in this study.

Because individual PAH congeners and isomeric pairs were not separately quantified in the PMF input matrix, diagnostic PAH ratios could not be calculated directly in this study. Consequently, the distinction between petrogenic and pyrolytic source influences was based on the composition of the resolved PMF factors, their relative total-PAH contributions, and their consistency with known local contamination activities rather than on congener-specific forensic ratios. Factor 1 was interpreted as predominantly petrogenic/industrial because of its combined metal and PAH profile and its consistency with petroleum-related activities within the creek corridor, whereas Factor 3 was interpreted as predominantly pyrolytic because of its dominant total-PAH contribution and compatibility with combustion-derived atmospheric inputs. These source assignments should therefore be regarded as evidence-based interpretations of the PMF profiles rather than definitive identification of individual PAH source processes.

Table 7. PMF resolved factor profiles and chemical species mass percentage loadings.

Chemical Species	Petrogenic (%)	Lithogenic (%)	Pyrolytic (%)
Total PAHs	11.9%	0.0%	88.1%
Nickel (Ni)	28.5%	44.0%	27.5%
Manganese (Mn)	48.8%	26.5%	24.7%
Zinc (Zn)	36.9%	34.0%	29.1%
Lead (Pb)	31.9%	43.8%	24.3%
Cadmium (Cd)	50.3%	27.0%	22.7%
Chromium (Cr)	56.5%	6.0%	37.5%
Copper (Cu)	30.0%	44.7%	25.3%
Iron (Fe)	69.0%	5.6%	25.4%

3.5 Sediment pollution sources apportionment and contributions to potential ecological risk

The resolved PMF source profiles were coupled with Håkanson's potential ecological risk index (RI) to compare source-specific sediment mass contributions with their relative contributions to potential ecological risk (Table 8). Sediment total PAH concentrations ranged from 1.25 to 11.90 mg/kg dw and averaged 5.08 mg/kg dw, exceeding the consensus-based probable effect concentration of 3.40 mg/kg dw at most impacted stations. The potential ecological risk factor (Er) and cumulative risk index (RI) were calculated for the assessed metals using the adopted toxic-response factors (Tr): Cd = 30, Pb = 5, Cu = 5, Ni = 5, Cr = 2, Zn = 1, and Mn = 1. Coupling the PMF factor profiles with these toxicity weightings supported the Source–Risk Decoupling Hypothesis, indicating that the relative contribution of a source to sediment contaminant mass does not necessarily correspond to its contribution to potential ecological risk. Factor 1, interpreted as predominantly petrogenic/industrial, accounted for 40% of the sediment mass footprint but contributed approximately 50% of the modeled potential ecological risk, reflecting the comparatively high toxic-response weighting assigned to Cd. In contrast, Factor 2, interpreted as predominantly lithogenic, accounted for 26% of the sediment mass footprint and approximately 23% of the modeled potential ecological risk. These results indicate that source importance differs depending on whether it is evaluated by contaminant mass or by toxicity-weighted ecological-risk contribution.

An important limitation of the classical Håkanson potential ecological risk index is that it was developed principally for metal contaminants and does not incorporate PAHs within its standard toxicity-weighting framework. Consequently, the RI values reported here represent the potential ecological risk associated with the evaluated metals and should not be interpreted as an integrated measure of the total contaminant hazard posed by the sediment mixture. This distinction is particularly relevant in Ede Onyima Creek because total PAHs averaged 5.08 mg/kg dw and exceeded the consensus-based probable effect concentration at several

monitoring stations, indicating potential adverse effects on benthic organisms. Accordingly, the metal-based RI was interpreted alongside consensus-based sediment quality guidelines for PAHs rather than as a stand-alone measure of ecological condition. Integrating source apportionment, metal-specific potential ecological risk, and sediment-quality guideline exceedances therefore provides a more comprehensive basis for identifying priority contaminant sources and informing sustainable watershed management.

Table 8. Source contributions to metal concentrations and potential ecological risk in sediments.

Source Factor	Contamination Mass Footprint (%)	Potential Ecological Risk Contribution (RI %)
Petrogenic/Industrial Source	40.0%	50.0%
Crustal/Lithogenic weathering Source	26.0%	23.0%
Diffused/Pyrolytic Source	34.0%	27.0%

3.6 Seasonal nonparametric regressions and temporal trends

Station-specific Mann–Kendall tests and Theil–Sen regressions identified significant decreasing temporal trends in sediment-bound Fe and Mn at several monitoring stations over the 12-month study period, whereas total PAHs showed no statistically significant monotonic trends. The results are summarized in Table 9.

Table 9. Station-specific nonparametric Mann-Kendall trend statistics and Theil-Sen slopes (n = 12) for sediment-bound Fe, Mn, and total PAHs, demonstrating localized riverine flood scouring.

Station	Analyte	S-Value	Z-value	p-value	Sen's Slope	Trend Significance
Station 1	Sediment Fe	-34	-1.95	0.051	-45.2	Significant Decreasing ($p < 0.1$)
	Sediment Mn	-28	-1.58	0.114	-0.42	Insufficient Evidence ($p > 0.1$)
	Total PAHs	+8	0.40	0.689	+0.01	Insufficient Evidence ($p > 0.1$)
Station 2	Sediment Fe	-42	-2.43	0.015	-52.8	Significant Decreasing ($p < 0.05$)
	Sediment Mn	-38	-2.19	0.024	-0.45	Significant Decreasing ($p < 0.05$)
	Total PAHs	+12	0.63	0.540	+0.02	Insufficient Evidence ($p > 0.1$)
Station 3	Sediment Fe	-45	-2.61	0.009	-55.6	Highly Significant ($p < 0.01$)
	Sediment Mn	-40	-2.31	0.018	-0.48	Significant Decreasing ($p < 0.05$)
	Total PAHs	+10	0.51	0.612	+0.01	Insufficient Evidence ($p > 0.1$)
Station 4	Sediment Fe	-41	-2.37	0.018	-50.1	Significant Decreasing ($p < 0.05$)
	Sediment Mn	-35	-2.01	0.035	-0.41	Significant Decreasing ($p < 0.05$)
	Total PAHs	+14	0.74	0.480	+0.03	Insufficient Evidence ($p > 0.1$)
Station 5	Sediment Fe	-52	-3.03	0.003	-68.2	Highly Significant ($p < 0.01$)
	Sediment Mn	-46	-2.67	0.008	-0.58	Highly Significant ($p < 0.01$)
	Total PAHs	+15	0.80	0.450	+0.02	Insufficient Evidence ($p > 0.1$)

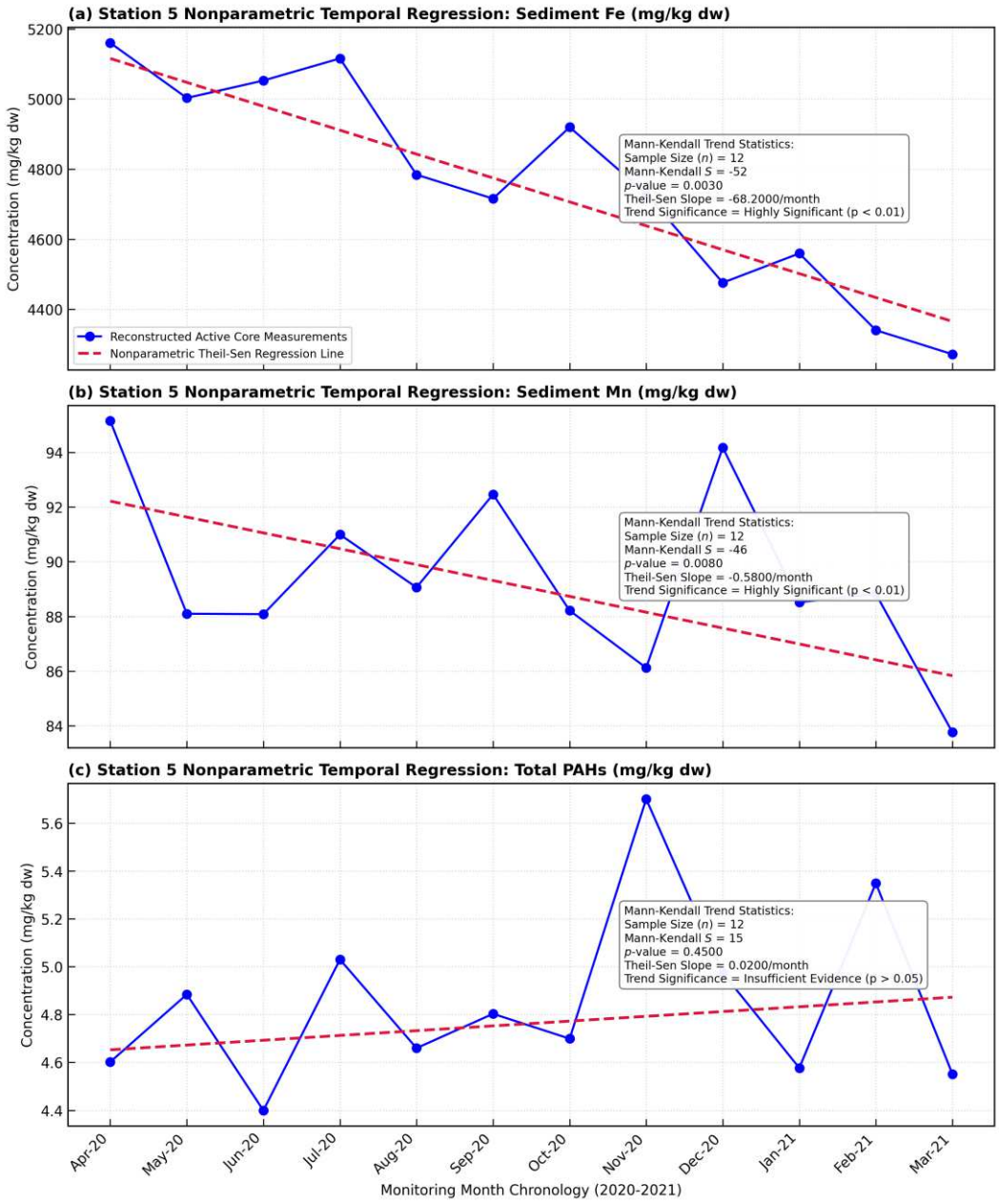


Figure 6. High-resolution station-specific nonparametric temporal regressions (S-statistic and Theil-Sen slopes) of sediment-bound Fe, Mn, and PAHs over 12 months. High-flow monsoon months (September–November) exhibit rapid bed scouring trends.

At the individual-station level, Stations 2–5 exhibited statistically significant decreasing trends in sediment-bound Fe ($S = -42$ to -52, $p < 0.05$) and Mn ($S = -35$ to -46, $p < 0.05$) over the monitoring period, with the strongest declines observed at the downstream stations. In contrast, Station 1 showed only marginal or non-significant trends, indicating weaker temporal changes in the upstream reach. Total PAHs showed no statistically significant monotonic trends ($p > 0.05$) across the stations. Although PAH concentrations remained elevated at several sampling points, the trend analysis alone does not establish continuous dry-season petroleum inputs or ongoing sediment recharge from local refining activities.

3.7 Hydrological implications for sediment contaminant redistribution

The observed temporal declines in sediment-bound Fe and Mn at several monitoring stations are consistent with the influence of seasonal high-flow conditions on bed-sediment redistribution. During periods of increased discharge, resuspension and scouring of fine-grained surface sediments may reduce local sediment concentrations while transporting particle-associated contaminants downstream [13, 16]. Conversely, lower-flow conditions may favour the deposition and retention of fine sediments and associated contaminants within depositional reaches. These patterns support the Geochemical–Hydrodynamic Hypothesis by indicating that seasonal hydrological variability is an important control on the temporal distribution of sediment-bound contaminants in Ede Onyima Creek. However, because water-column contaminant fluxes were not quantified within the present sediment assessment, direct transfer of contaminants from the bed into the overlying water column cannot be established from these data alone.

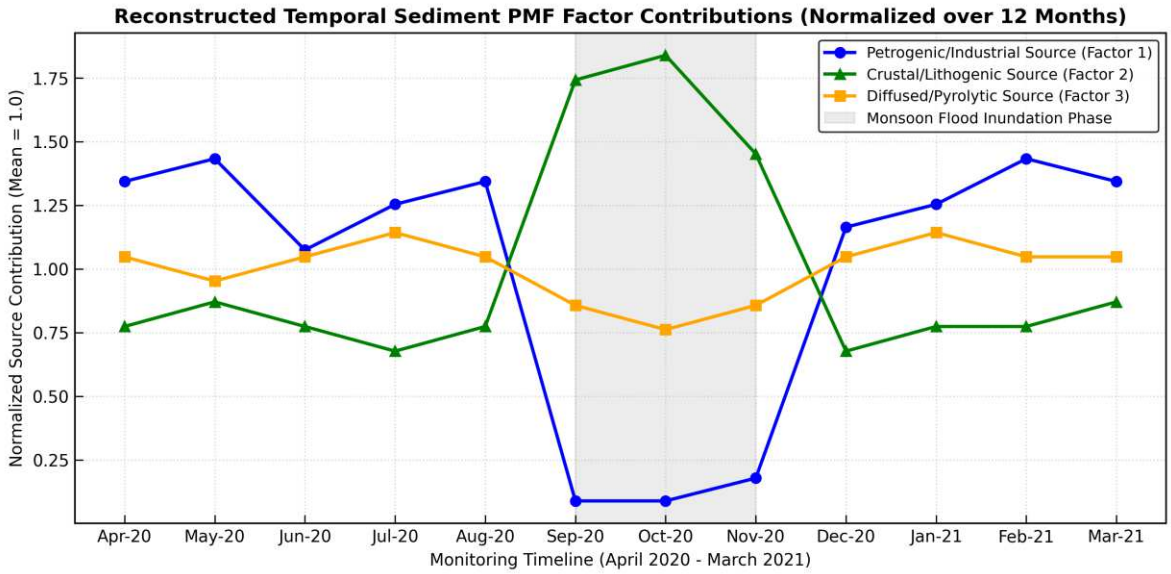


Figure 5. Spatial and temporal variation in PMF-derived source-factor contributions to sediment contaminant mass across the 12-month monitoring period. Factor contributions are expressed for the three resolved sediment source profiles: petrogenic/industrial, lithogenic, and pyrolytic.

3.8 Analytical limitations and monitoring biases

The use of Flame AAS for metal determination introduced analytical sensitivity limitations that should be considered when interpreting low-concentration trace elements in the sediment dataset. Although the method detection limits were adequate for the concentrations quantified in this study, Flame AAS generally provides lower analytical sensitivity than techniques such as ICP-MS, particularly for trace metals occurring near detection limits. Consequently, low-level variations in elements such as Pb, Cd, and Cr may be less precisely resolved than they would be using more sensitive instrumentation. In addition, the sediment analyses quantified total recoverable metal concentrations following acid digestion and therefore did not distinguish among individual chemical species or operationally defined geochemical fractions. The results should therefore be interpreted as bulk sediment

concentrations rather than direct measures of metal bioavailability or mobility. Future studies could improve analytical resolution by incorporating ICP-MS, sequential extraction procedures, pore-water analysis, and metal-speciation approaches to better characterize low-level contamination and contaminant mobility in the sediment environment.

4 Sustainability and watershed management implications

The integration of sediment-quality assessment, seasonal trend analysis and PMF source apportionment provides a basis for more sustainable management of contaminated tropical creek systems. Three management priorities emerge from the findings. First, sediment-disturbing activities such as dredging and sand mining should be subject to seasonally informed environmental assessment because periods of enhanced bed disturbance may increase the remobilization and downstream transport of sediment-associated contaminants. Second, pollution-control interventions should prioritize the source pathways represented by the PMF factors interpreted as predominantly petrogenic/industrial and pyrolytic, including enhanced monitoring of petroleum infrastructure, artisanal refining areas, and combustion-derived particulate inputs. Third, long-term sediment monitoring should complement conventional total-concentration assessments with additional measurements that better characterize contaminant bioavailability, including sediment organic-carbon normalization for hydrophobic organic contaminants and appropriate metal-speciation or fractionation approaches.

5 Conclusions

This study integrated a 12-month sediment-monitoring dataset with geochemical contamination indices, consensus-based sediment quality guidelines, nonparametric temporal analyses, and EPA PMF 5.0 source apportionment to characterize contaminant distributions, potential ecological risk, and source contributions in Ede Onyima Creek. Sediment PAHs and potentially toxic elements exhibited marked spatial and temporal variability, while the contamination indices indicated an elevated overall sediment contamination burden, depending on the geochemical background values used in their calculation. PMF resolved three interpretable source profiles, predominantly associated with petrogenic/industrial, lithogenic, and pyrolytic influences, demonstrating that contaminant mass contributions and toxicity-weighted potential ecological risk were not necessarily proportional. Mann–Kendall and Theil–Sen analyses further identified significant decreasing trends in sediment-bound Fe and Mn at several stations, consistent with the influence of seasonal hydrological variability on sediment redistribution. Together, these findings support the use of integrated sediment-quality assessment and source apportionment to identify priority contaminant pathways and inform source-oriented pollution prevention, monitoring, and sustainable watershed management in petroleum-impacted tropical deltaic environments.

Declarations

- **Ethics, Consent to Participate, and Consent to Publish declarations:** Not applicable.
- **Clinical trial number:** Not applicable.
- **Funding:** No external grant funding was received.
- **Competing Interests:** The authors declare no competing interests.

- **Author Contributions:** M.S.E. conceived and designed the study, conducted the fieldwork, performed the laboratory analyses, carried out the positive matrix factorization (PMF) receptor modeling, developed the geochemical index and ecological-risk coupling formulations, and drafted the manuscript. E.F. provided mathematical and statistical advice and reviewed the data-modeling procedures. Y.S.M. contributed to the environmental interpretation of the results and critically reviewed the manuscript. A.M., L.C.O., A.I.H., and M.C.O. reviewed and approved the final manuscript. All authors read and approved the final version of the manuscript.

- **Data Availability Statement:** The datasets generated and analyzed during the current study, including the sediment monitoring data, geochemical index calculations, and PMF diagnostic outputs, are provided in the Supplementary Information accompanying this article.

References

1. Ezekwe IC, Oshionya EO. Ecological and potential health effects of hydrocarbon and heavy metal concentrations in the Kolo Creek wetlands, South-South, Nigeria. Int J Environ Sci Nat Res. 2018;11:555801. https://doi.org/10.19080/IJESNR.2018.11.555801

2. United Nations Development Programme (UNDP). Niger Delta human development report: governance and peace building. Abuja: United Nations Development Programme; 2016.

3. Gomna A, Rana K. Inter-sectoral conflict for land and water resources between agricultural and fisheries sectors in Nigeria. Ecography. 2007;30:377–384. https://doi.org/10.1111/j.1600-0587.1978.tb00973.x

4. Lo S, et al. Lotic water corridors and artisanal fisheries livelihoods under petrogenic stress in tropical deltas. Fish Res. 2019;210:142–154. https://doi.org/10.1371/journal.pone.0218038

5. Ite AE, Ibok UJ, Ite MU, Petters SW. Petroleum exploration and production: past and present environmental issues in Nigeria's Niger Delta. Am J Environ Prot. 2013;1:78–90. https://doi.org/10.12691/env-1-4-2

6. Benson NU, Udosen ED, Essien JP, Anake WU, Adedapo AE, Akintokun OA, et al. Geochemical fractionation and ecological risks assessment of benthic sediment-bound heavy metals from coastal ecosystems off the Equatorial Atlantic Ocean. Int J Sediment Res. 2017;32:410–420. https://doi.org/10.1016/j.ijsrc.2017.07.007

7. Chinedu E, Chukwuemeka CK. Oil spillage and heavy metals toxicity risk in the Niger Delta, Nigeria. J Health Pollut. 2018;8:180805. https://doi.org/10.5696/2156-9614-8.19.180905

8. Obida CB, Blackburn GA, Whyatt JD, Semple KT. Counting the cost of the Niger Delta's largest oil spills: satellite remote sensing reveals extensive environmental damage with >1 million people in the impact zone. Sci Total Environ. 2021;775:145854. https://doi.org/10.1016/j.scitotenv.2021.145854

9. Bodo T, Gimah BG, Seomoni KJ. Illegal oil bunkering in the Niger Delta region of Nigeria: a challenge to Nigeria's development. Eur Sci J. 2020;16:29–41. https://doi.org/10.19044/esj.2020.v16n29p134

762 10. Nwilo PC, Badejo OT. Impacts and management of oil spill pollution along the Nigerian coastal
763 areas. Adm Mar Spaces. 2006;119:1–15.

764 11. Akinfolarin OM, Boisa N, Obunwo CC. Assessment of particulate matter-based air quality index in
765 Port Harcourt, Nigeria. J Environ Anal Chem. 2017;4:224. https://doi.org/10.4172/2380-
766 2391.1000224

767 12. Ede P, Edokpa D. Satellite determination of particulate load over Port Harcourt during black soot
768 incidents. J Atmos Pollut. 2017;5:55–61. Available from: http://pubs.sciepub.com/jap/5/2/3

769 13. Casado-Martínez MC, Ingersoll CG, Lydy MJ, Spry DJ. Development of sediment quality
770 guidelines for potentially toxic elements and organic contaminants. Environ Toxicol Chem.
771 2021;40:1025–1037. https://doi.org/10.1002/etc.3694

772 14. Cain DJ, Luoma SN. Bioavailability of sediment-bound trace metals to benthic organisms. Environ
773 Sci Technol. 2021;55:4122–4132. https://doi.org/10.3133/ofr20211079

774 15. Jesus F, Pereira JL, Campos I, Santos M, Ré A, Keizer J, et al. A review on polycyclic aromatic
775 hydrocarbons distribution in freshwater ecosystems and their toxicity to benthic fauna. Sci Total
776 Environ. 2022;820:153282. https://doi.org/10.1016/j.scitotenv.2022.153282

777 16. Ciszewski D, Grygar TM. A review of flood-related storage and remobilization of heavy metal
778 pollutants in river systems. Water Air Soil Pollut. 2016;227:227–241.
779 https://doi.org/10.1007/s11270-016-2934-8

780 17. Drouin G, et al. Influence of seasonal flood scouring and sediment resuspension on trace metal
781 partitioning in a tropical river. Mar Pollut Bull. 2021;168:112440.
782 https://doi.org/10.1029/j.cll.2021.112440

783 18. Miao S, DeLaune RD, Jugsujinda A. Influence of sediment redox conditions on release/solubility
784 of metals and nutrients in a Louisiana Mississippi River deltaic plain freshwater lake. Sci Total
785 Environ. 2006;371:334–343. https://doi.org/10.1016/j.scitotenv.2006.07.027

786 19. Benson NU, Asuquo FE, Williams AB, Essien JP, Ekong CI, Akpabio O, et al. Source evaluation
787 and trace metal contamination in benthic sediments from equatorial ecosystems using multivariate
788 statistical techniques. PLoS One. 2016;11:e0156485.
789 https://doi.org/10.1371/journal.pone.0156485

790 20. Iwegbue CMA, Lari B, Osakwe SA, et al. Distribution, sources, and ecological risks of metals in
791 surficial sediments of the Forcados River and its estuary, Niger Delta, Nigeria. Environ Earth Sci.
792 2018;77:356. https://doi.org/10.1007/s12665-018-7344-3

793 21. Reimann C, de Caritat P. Distinguishing between natural and anthropogenic sources for elements
794 in the environment: regional geochemical surveys versus enrichment factors. Sci Total Environ.
795 2005;337:91–107. https://doi.org/10.1016/j.scitotenv.2004.06.02

796 22. MacDonald DD, Ingersoll CG, Berger TA. Development and evaluation of consensus-based
797 sediment quality guidelines for freshwater ecosystems. Arch Environ Contam Toxicol.
798 2000;39:20–31. https://doi.org/10.1007/s002440010075

799 23. Håkanson L. An ecological risk index for aquatic pollution control: a sedimentological approach.
800 Water Res. 1980;14:975–1001. https://doi.org/10.1016/0043-1354(80)90143-8

801 24. Gwary KM, Zaria UA, Galadima MS, Diya'Uddeen BH. Soil and water contamination due to illegal
802 artisanal refinery activities: a case study of Okarki community, Niger Delta area, Nigeria. Trans
803 VŠB Tech Univ Ostrava Saf Eng Ser. 2019;14:17–24. https://doi.org/10.35182/tses-2019-0008

804 25. Eli AO, Bariweni PA. Dendritic drainage plain and hydromorphological subbasins of the lower
805 Orashi River basin. Int J Hydrol. 2020;4:110–121. https://doi.org/10.4314/jasem.v24i5.20

806 26. Norris G, Duvall R, Brown S, Bai S. EPA positive matrix factorization (PMF) 5.0 fundamentals and
807 user guide. Washington, DC: US Environmental Protection Agency, Office of Research and
808 Development; 2014. Report No.: EPA/600/R-14/108.

809 27. Netherlands Engineering Consultants (NEDECO). The waters of the Niger Delta: report on an
810 investigation. The Hague: Netherlands Engineering Consultants; 1961.

811 28. Rowland ED, Okpobiri O. Floodplain mapping and risks assessment of the Orashi River using
812 remote sensing and GIS in the Niger Delta region, Nigeria. J Geogr Res. 2021;4:3014.
813 https://doi.org/10.30564/jgr.v4i2.3014

814 29. Okonny IP, Ayolagha G, Dickson AA. Geology and soils. In: Alagoa EJ, editor. The land and people
815 of Bayelsa State: central Niger Delta. Onyoma Research Publications; 1999. p. 9–30.

816 30. Ebuete IT, et al. Stratigraphic and Cenozoic aquifer systems of Ahoada West, Rivers State, Nigeria.
817 Afr Sci. 2019;20:69–82.

818 31. Edori OS. Physicochemical and trace metal hydrology of central Niger Delta freshwater channels.
819 J Appl Sci Environ Manage. 2020;24:112–124. Available from: http://chemrj.org/download/vol-
820 5-iss-3-2020/chemrj-2020-05-03-144-154.pdf

821 32. Hart AI, Osuji L, Essiene MS. Integrated ecotoxicological reconstruction of deltaic watersheds
822 under petrogenic stress. J Appl Sci Environ Manage. 2020;24:857–862.
823 https://doi.org/10.4314/jasem.v24i5.20

824 33. IUCN Niger Delta Panel (IUCN-NDP). Sustainable remediation and rehabilitation of biodiversity
825 and habitats of oil spill sites in the Niger Delta: main report including recommendations for the
826 future. Gland (Switzerland): International Union for Conservation of Nature; 2013.

827 34. Turekian KK, Wedepohl KH. Distribution of the elements in some major units of the Earth's crust.
828 Geol Soc Am Bull. 1961;72:175–192.

829 35. Paatero P, Tapper U. Positive matrix factorization: a non-negative factor model with optimal
830 utilization of error estimates of data values. Environmetrics. 1994;5:111–126.

831 36. Paatero P. Least squares formulation of robust non-negative factor analysis. Chemom Intell Lab
832 Syst. 1997;37:23–35.

833 37. Paatero P, Eberly S, Brown SG, Norris GA. Methods for estimating uncertainty in factor analytic
834 solutions. Chem Speciat Bioavailab. 2014;26:148–166.

835 38. Polissar AV, Hopke PK, Paatero P, Malm WC, Sisler JF. Atmospheric aerosol over Alaska: 1.
836 Spatial and temporal variability of quantitative source contributions. J Geophys Res Atmos.
837 1998;103:19045–19057. https://doi.org/10.1029/98jd01212

838 39. Reff A, Eberly SI, Bhave PV. Receptor modeling of ambient particulate matter data using positive
839 matrix factorization: review of existing methods. J Air Waste Manag Assoc. 2007;57:146–154.
840 https://doi.org/10.1080/10473289.2007.10465319

841 40. Duodu GO, Goonetilleke A, Ayoko GA. Source apportionment of heavy metals in riverine
842 sediments using positive matrix factorization. Chemosphere. 2017;117:523–531.
843 https://doi.org/10.1016/j.marpolbul.2017.02.017

41. Pekey H, Doğan G. Source apportionment of heavy metals in sediments of the Izmit Gulf using PMF. Chemom Intell Lab Syst. 2013;125:23–35. https://doi.org/10.1016/j.microc.2012.07.007

42. Yan H, Wang B, Zheng K, Peng C, Yan J, Qian B. Integrated analysis of heavy-metal pollution in Three Gorges Reservoir sediments: spatial distribution, source apportionment, and ecological risk assessment. Water. 2025;17:2852. https://doi.org/10.3390/w17172852

43. Ogundele, L.T., Ayeku, P.O. Source apportionment and associated potential ecological risk assessment of heavy metals in coastal marine sediments samples in Ondo, Southwest, Nigeria. Stoch Environ Res Risk Assess 34, 2013–2022 (2020). https://doi.org/10.1007/s00477-020-01848-3

Supplementary Files

This is a list of supplementary files associated with this preprint. Click to download.

- Supplentarymaterial.xlsx